Higgs pair production in the ElectroWeak Chiral Lagrangian framework

Matteo Capozi
G. Buchalla, A. Celis, G. Heinrich, L. Scyboz [arXiv:1806.05162]

Max-Planck-Institut für Physik

26/09/2018
Particle Physics Challenges - DESY
Hamburg

Motivations

- No evidences of new physics have been found yet.
- New physics may hide at higher scales, therefore an Effective Field Theory (EFT) can allow us to parametrize new physics contributions.
- We work in the non-linear EFT framework provided by the ElectroWeak Chiral Lagrangian (EWChL) [Buchalla et al. arXiv:1307.5017].
- Many of the Higgs couplings are well constrained already or can be obtained from other processes, but this is not true for the Higgs boson self coupling.
- We focus on the gg to HH process.

$$L_{gg\to hh} \supset -m_t \bar{t}t \left(c_t \frac{h}{v} + c_{tt} \frac{h^2}{2v^2} \right) - c_{hhh} \frac{1}{6} \left(\frac{3m_h^2}{v} \right) h^3 + \frac{g_s^2}{16\pi^2} \langle G_{\mu\nu} G^{\mu\nu} \rangle \left(c_{ggh} \frac{h}{v} + c_{gghh} \frac{h^2}{2v^2} \right)$$

EWChL for gg→HH

- At leading order there are 5 different diagrams: 2 SM-like diagrams and 3 totally new diagrams.

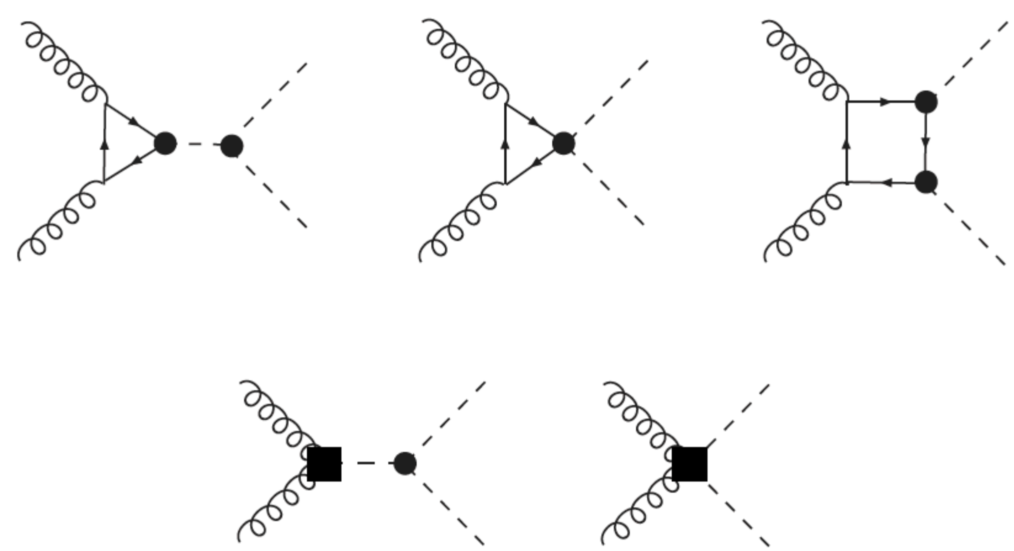

- The Feynman amplitude of this process can be written as: $\boxed{M^{\mu\nu} = F_1 T_1^{\mu\nu} + F_2 T_2^{\mu\nu}}$

$$T_1^{\mu\nu} = -g^{\mu\nu} + \frac{k_1^\nu k_2^\mu}{(k_1 \cdot k_2)} \qquad T_2^{\mu\nu} = g^{\mu\nu} + \frac{1}{k_T^2 (k_1 \cdot k_2)} \left(m_h^2 k_1^\nu k_2^\mu - 2(k_1 \cdot k_3) k_3^\nu k_2^\mu - 2(k_2 \cdot k_3) k_3^\mu k_1^\nu \right) + 2(k_1 \cdot k_2) k_3^\mu k_3^\nu \Big)$$

- In order to compute the deviations of the model, we need to know the contributions of these new diagrams to the form factors F_1 and F_2.

$$\hat{\sigma}^{LO} = \frac{\alpha_s^2}{2^{12} v^4 (2\pi)^3 \hat{s}^2} \int_{\hat{t}_-}^{\hat{t}^+} d\hat{t} \{ |F_1|^2 + |F_2|^2 \}$$

gg→HH contributions in the EWChL framework

Leading order

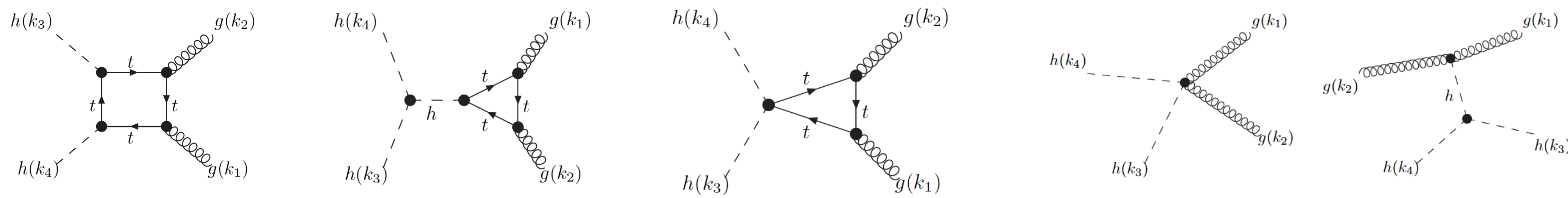

NLO QCD virtual

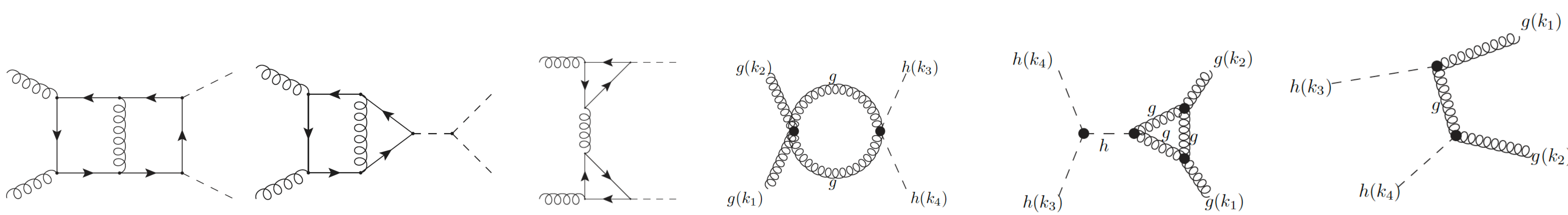

$+\ldots$

Borowka et al. arXiv:1608.04798

NLO QCD real

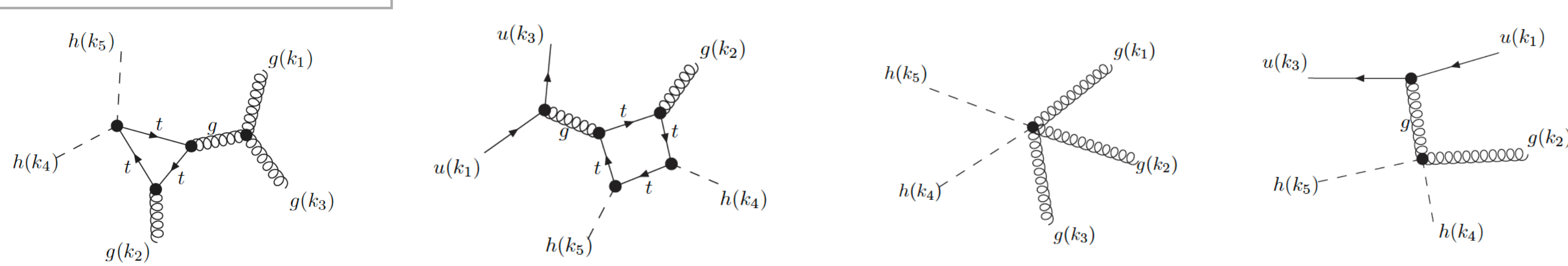

$+\ldots$

Method of the calculation

- In order to obtain the LO QCD cross section and the NLO QCD real corrections we used a C++ code linked to GoSam [Cullen et al. arXiv:1404.7096].

- For the NLO QCD virtual correction we used the two-loop integrals computed numerically for the SM (using the program SecDec) case [Borowka et al. arXiv:1608.04798] as far as possible and then manipulated the results using a python script.

- Within our setup we can produce the full top mass dependent NLO QCD cross section and differential distributions.

- In the following we will show distributions for some benchmark points and compare them with SM results.

Benchmark points

- Benchmark points introduced in Carvalho et al. [arXiv:1507.02245, arXiv:1608.06578 and arXiv:1710.08261], calculating LO distributions.
- According to the values of the five anomalous couplings the shape of the differential distribution can change.
- The idea of the benchmark points is to define 12 clusters with different shapes, which characterize distributions attributed to a given choice of couplings.
- We produced the inclusive and differential cross sections at NLO with full top mass dependence.

Benchmark	c_{hhh}	c_t	c_{tt}	c_{ggh}	c_{gghh}
1	7.5	1.0	−1.0	0.0	0.0
2	1.0	1.0	0.5	$-\frac{1.6}{3}$	−0.2
3	1.0	1.0	−1.5	0.0	$\frac{0.8}{3}$
4	−3.5	1.5	−3.0	0.0	0.0
5	1.0	1.0	0.0	$\frac{1.6}{3}$	$\frac{1.0}{3}$
6	2.4	1.0	0.0	$\frac{0.4}{3}$	$\frac{0.2}{3}$
7	5.0	1.0	0.0	$\frac{0.4}{3}$	$\frac{0.2}{3}$
8a	1.0	1.0	0.5	$\frac{0.8}{3}$	0.0
9	1.0	1.0	1.0	−0.4	−0.2
10	10.0	1.5	−1.0	0.0	0.0
11	2.4	1.0	0.0	$\frac{2.0}{3}$	$\frac{1.0}{3}$
12	15.0	1.0	1.0	0.0	0.0
SM	1.0	1.0	0.0	0.0	0.0

Benchmark points

Benchmark	σ_{NLO} [fb]	K-factor	scale uncert. [%]	stat. uncert. [%]	$\frac{\sigma_{NLO}}{\sigma_{NLO,SM}}$
B_1	194.89	1.88	$^{+19}_{-15}$	1.6	5.915
B_2	14.55	1.88	$^{+5}_{-13}$	0.56	0.4416
B_3	1047.37	1.98	$^{+21}_{-16}$	0.15	31.79
B_4	8922.75	1.98	$^{+19}_{-16}$	0.39	270.8
B_5	59.325	1.83	$^{+4}_{-15}$	0.36	1.801
B_6	24.69	1.89	$^{+2}_{-11}$	2.1	0.7495
B_7	169.41	2.07	$^{+9}_{-12}$	2.2	5.142
B_{8a}	41.70	2.34	$^{+6}_{-9}$	0.63	1.266
B_9	146.00	2.30	$^{+22}_{-16}$	0.31	4.431
B_{10}	575.86	2.00	$^{+17}_{-14}$	3.2	17.48
B_{11}	174.70	1.92	$^{+24}_{-8}$	1.2	5.303
B_{12}	3618.53	2.07	$^{+16}_{-15}$	1.2	109.83
SM	32.95	1.66	$^{+14}_{-13}$	0.1	1

- Some of them already ruled out [arXiv:1806.00408, ATLAS-CONF-2018-043].

Benchmark points: m_{hh} and $p_{T,h}$ distributions

Benchmark 8-a

$$\frac{\sigma_{NLO}}{\sigma_{NLO,SM}} = 1.266$$

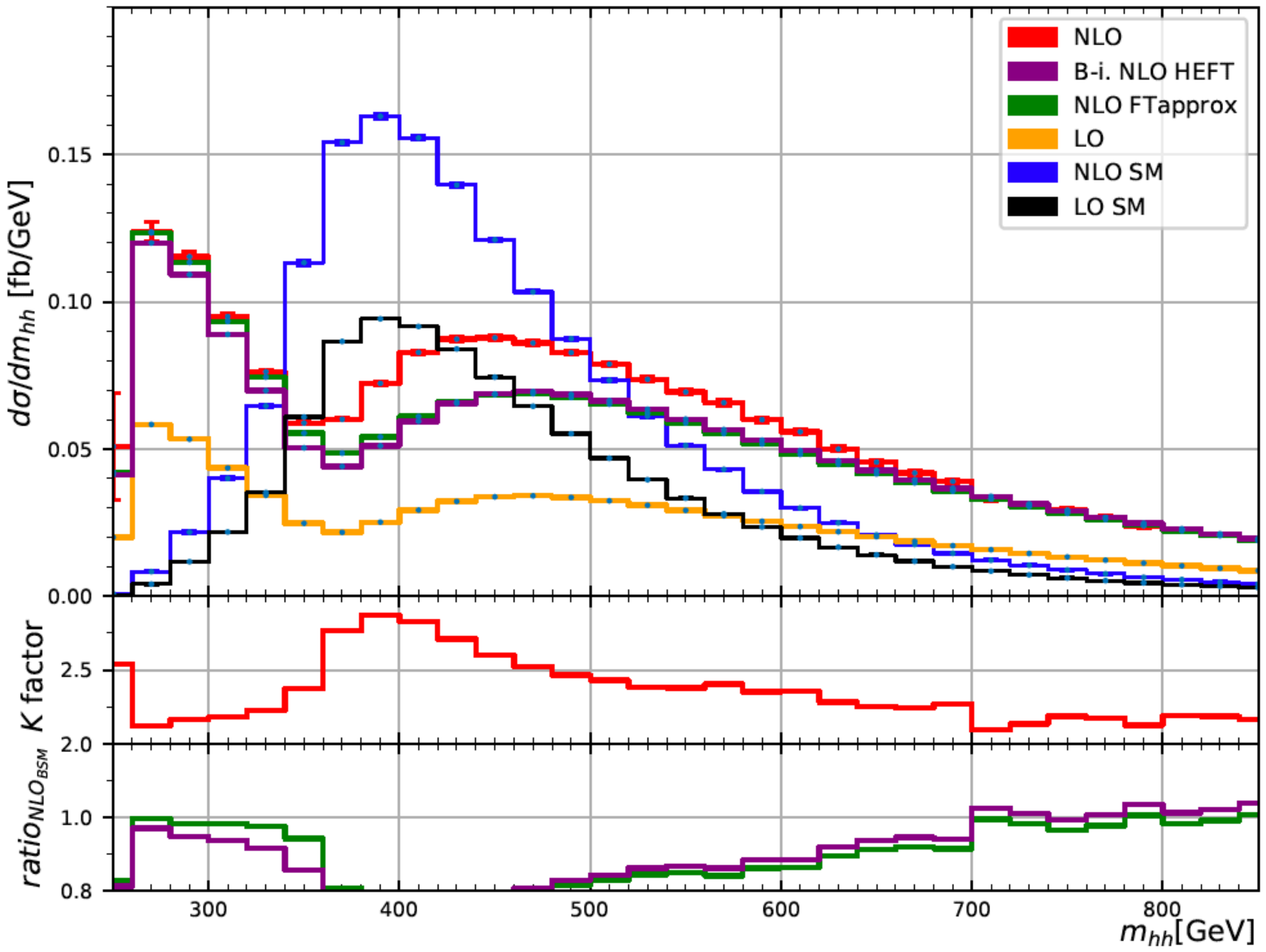

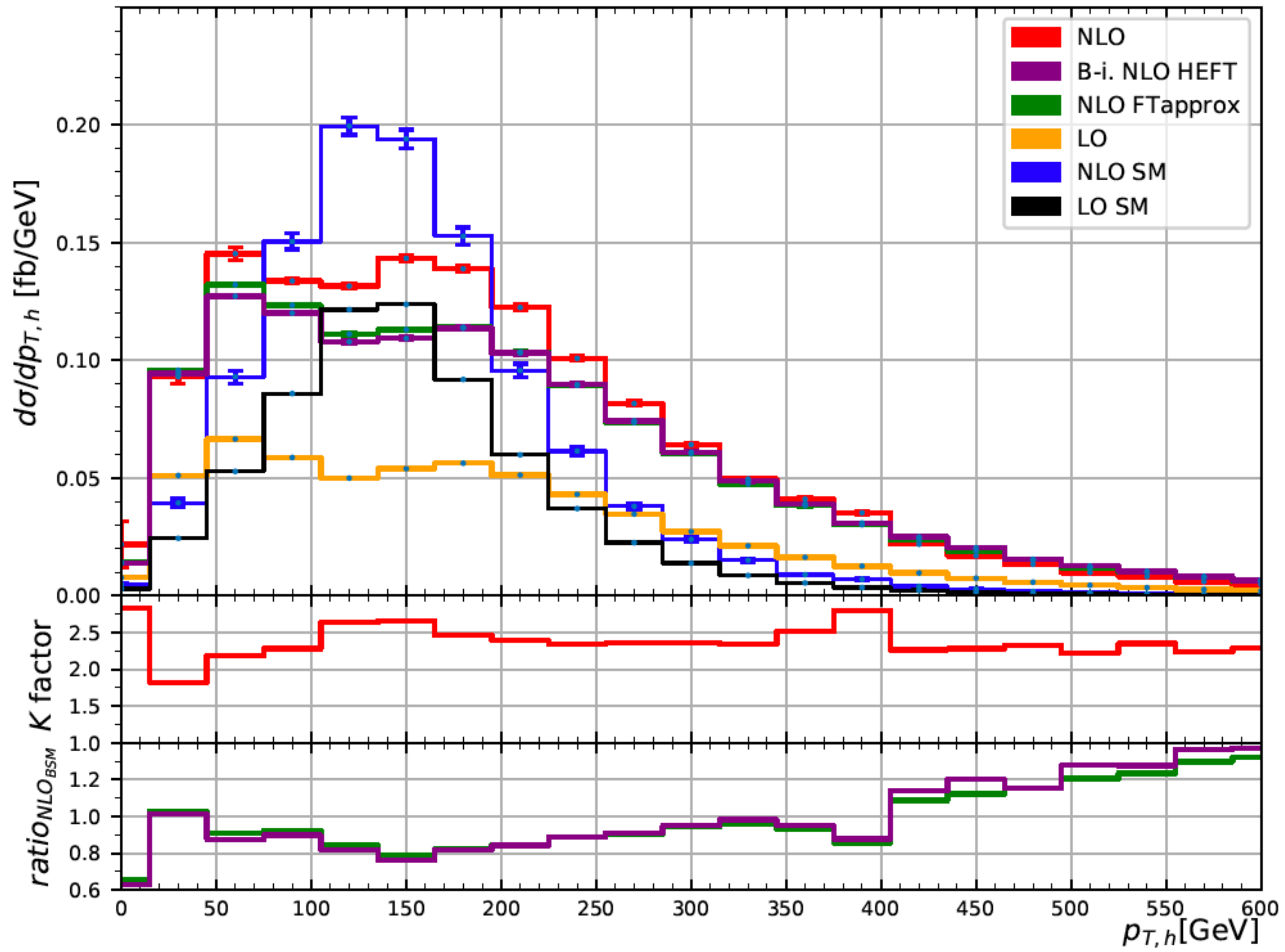

$$c_{hhh} = 1.0, c_t = 1.0, c_{tt} = 0.5, c_{ggh} = \frac{0.8}{3}, c_{gghh} = 0$$

Cross section parametrization

- In general the LO cross section for the process can be parametrized as function of the 5 BSM couplings in terms of 15 parameters.

$$\frac{\sigma_{LO}}{\sigma_{LO,SM}} = [A_1 c_t^4 + A_2 c_{tt}^2 + A_3 c_{thh}^2 c_{hhh}^2 + A_4 c_{ghh}^2 c_{hhh}^2 + A_5 c_{gghh}^2 + A_6 c_{tt} c_t^2 + A_7 c_t^3 c_{hhh}$$
$$+ A_8 c_{tt} c_t c_{hhh} + A_9 c_{tt} c_{ggh} c_{hhh} + A_{10} c_{tt} c_{cgghh} + A_{11} c_t^2 c_{ggh} c_{hhh} + A_{12} c_t^2 c_{gghh}$$
$$+ A_{13} c_t c_{hhh}^2 c_{ghh} + A_{14} c_t c_{hhh} c_{gghh} + A_{15} c_{ggh} c_{hhh} c_{gghh}]$$

- We determined the value of the 15 parameters via projections.
- We checked our results with the ones of Azatov et al. [arXiv:1502.00539] and found agreement.
- At NLO QCD the 15 coefficients change plus there are 8 new ones.

$$\frac{\sigma_{NLO}}{\sigma_{NLO,SM}} = [A'_1 c_t^4 + A'_2 c_{tt}^2 + A'_3 c_{thh}^2 c_{hhh}^2 + A'_4 c_{ghh}^2 c_{hhh}^2 + A'_5 c_{gghh}^2 + A'_6 c_{tt} c_t^2 + A'_7 c_t^3 c_{hhh}$$
$$+ A'_8 c_{tt} c_t c_{hhh} + A'_9 c_{tt} c_{ggh} c_{hhh} + A'_{10} c_{tt} c_{cgghh} + A'_{11} c_t^2 c_{ggh} c_{hhh} + A'_{12} c_t^2 c_{gghh}$$
$$+ A'_{13} c_t c_{hhh}^2 c_{ghh} + A'_{14} c_t c_{hhh} c_{gghh} + A'_{15} c_{ggh} c_{hhh} c_{gghh} + \underline{A'_{16} c_t^3 c_{ggh} + A'_{17} c_t c_{tt} c_{ggh}}$$
$$\underline{+ A'_{18} c_t c_{ggh}^2 c_{hhh} + A'_{19} c_t c_{ggh} c_{gghh} + A'_{20} c_t^2 c_{ggh}^2 + A'_{21} c_{tt} c_{ggh}^2 + A_{22} c_{ggh}^3 c_{hhh} + A'_{23} c_{ggh}^2 c_{gghh}}]$$

Cross section fit

A coeff	LO value	LO uncertainty	NLO value	NLO uncertainty
A_1	2.08059	0.00163127	2.23389	0.0100989
A_2	10.2011	0.00809032	12.4598	0.0424131
A_3	0.27814	0.00187658	0.342248	0.0153637
A_4	0.314043	0.000312416	0.346822	0.00327358
A_5	12.2731	0.0101351	13.0087	0.0962361
A_6	−8.49307	0.00885261	−9.6455	0.0503776
A_7	−1.35873	0.00148022	−1.57553	0.0136033
A_8	2.80251	0.0130855	3.43849	0.0771694
A_9	2.48018	0.0127927	2.86694	0.0772341
A_{10}	14.6908	0.0311171	16.6912	0.178501
A_{11}	−1.15916	0.00307598	−1.25293	0.0291153
A_{12}	−5.51183	0.0131254	−5.81216	0.134029
A_{13}	0.560503	0.00339209	0.649714	0.0287388
A_{14}	2.47982	0.0190299	2.85933	0.193023
A_{15}	2.89431	0.0157818	3.14475	0.148658
A_{16}			−0.00816241	0.000224985
A_{17}			0.0208652	0.000398929
A_{18}			0.0168157	0.00078306
A_{19}			0.0298576	0.000829474
A_{20}			−0.0270253	0.000701919
A_{21}			0.0726921	0.0012875
A_{22}			0.0145232	0.000703893
A_{23}			0.123291	0.00650551

- We present the results for the coefficients at LO and NLO.
- Using the fitted cross section we study the behavior of the cross section as a function of the BSM parameters.
- We show some of the iso-contours produced using the fit.

NLO Iso-contours

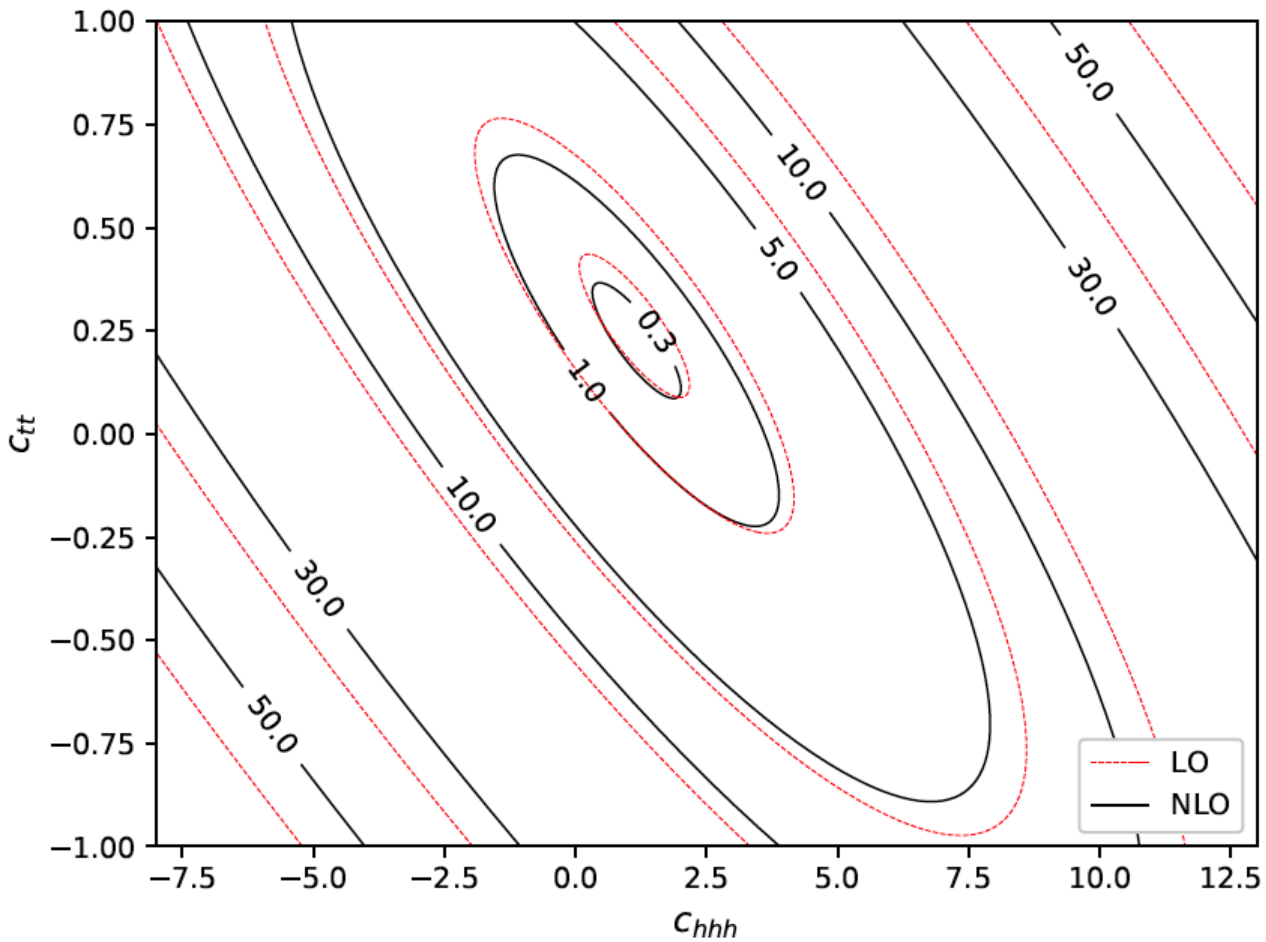

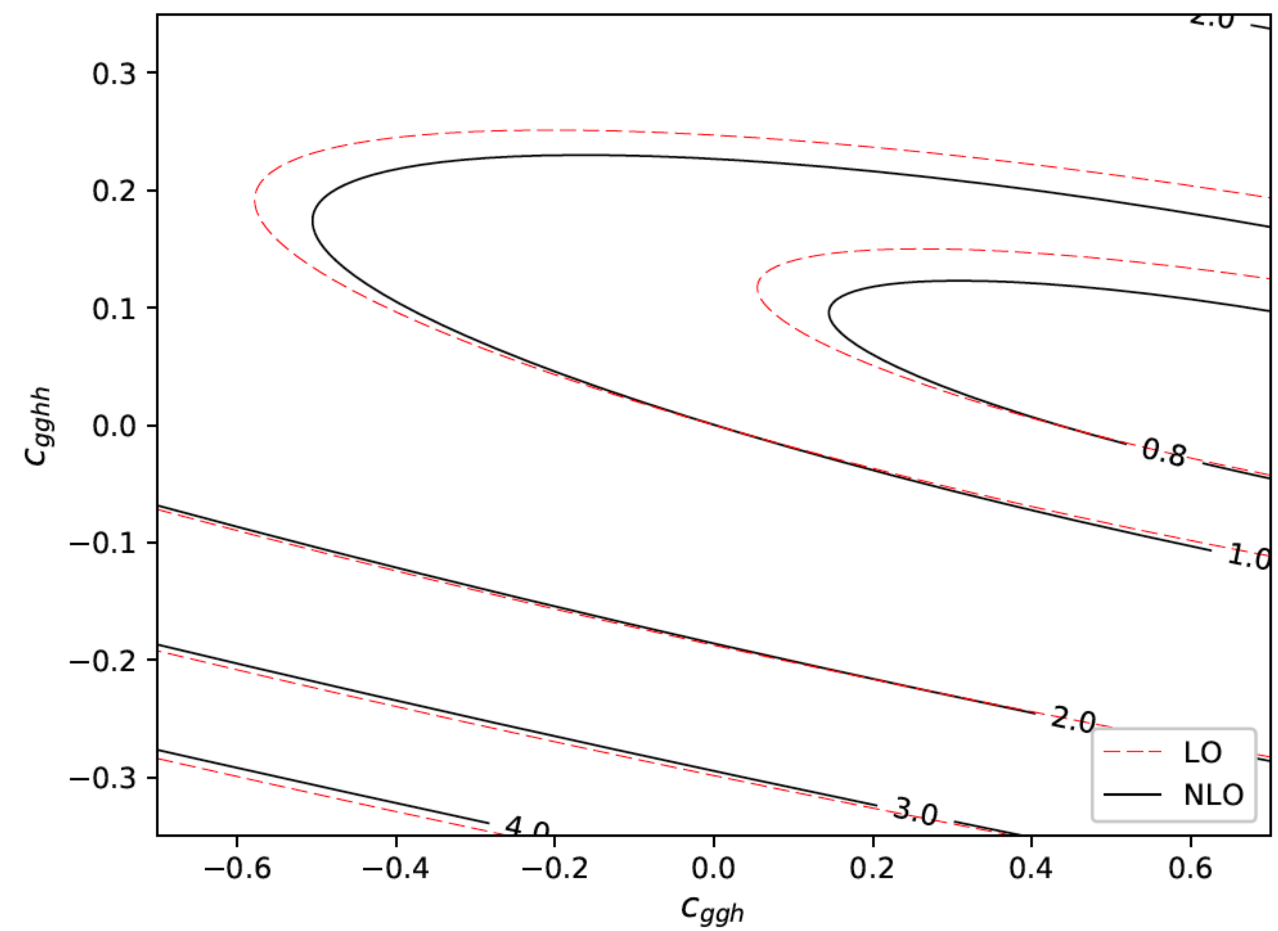

NLO 3D plots

- We performed the parametrization also at differential level, attached as ancillary files to 1806.05162.
- We used the differential fit to produce 3D plots.
- From the 3D plot one can understand the behavior of the differential distribution changing one of the BSM parameters.
- We made a study of the behavior of the differential m_{hh} cross section as a function of the 3 couplings which are difficult to constrain from other processes.
- In each plot we varied just one coupling in a range allowed by experimental constraints, fixing the others to the SM values.

NLO 3D plots

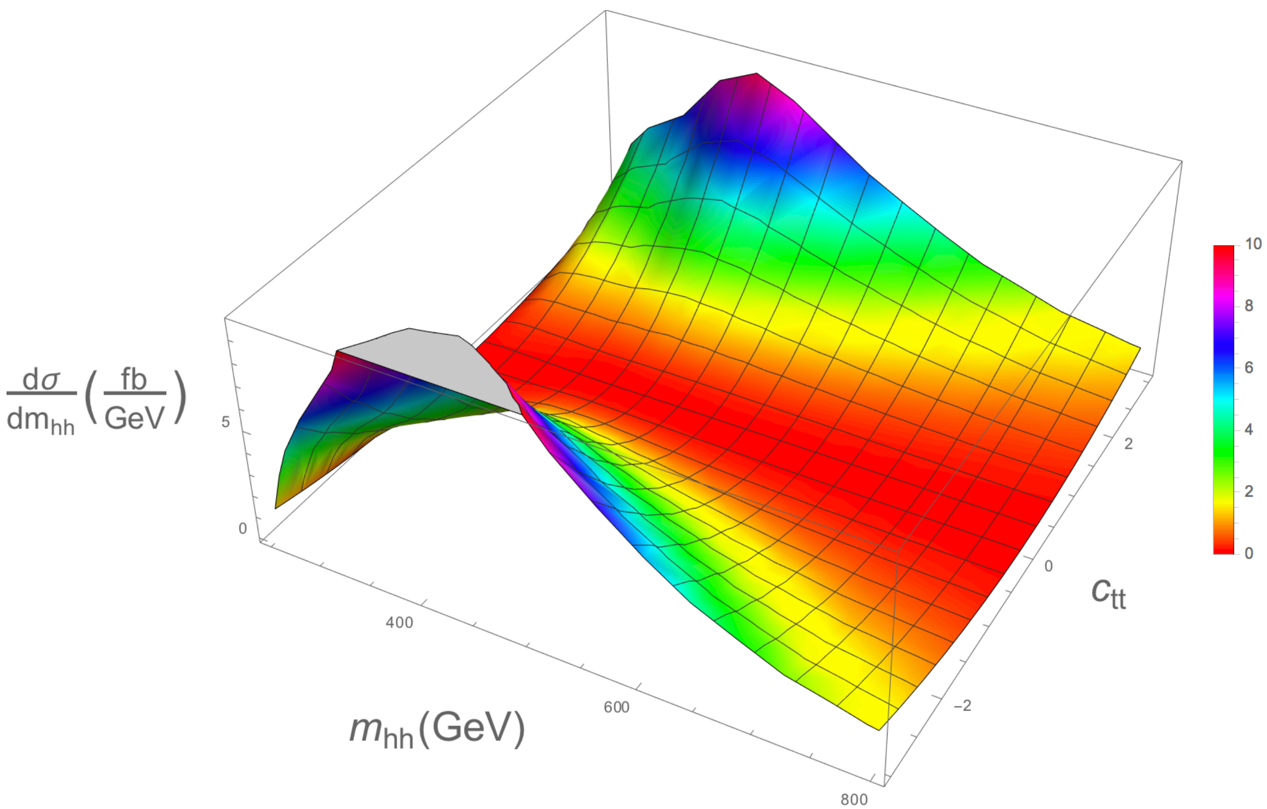
$\frac{d\sigma}{dm_{hh}}\left(\frac{fb}{GeV}\right)$
m_{hh}(GeV)
c_{tt}

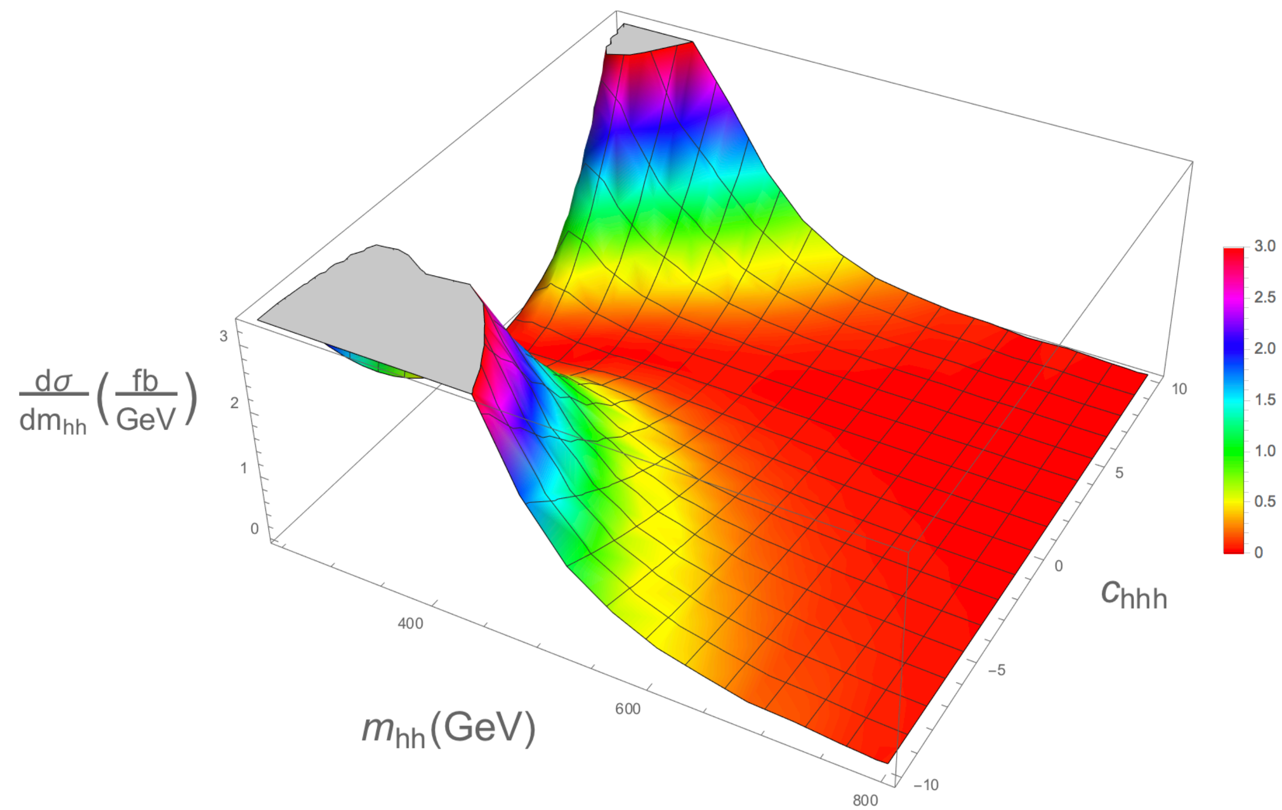
$\frac{d\sigma}{dm_{hh}}\left(\frac{fb}{GeV}\right)$
m_{hh}(GeV)
c_{hhh}

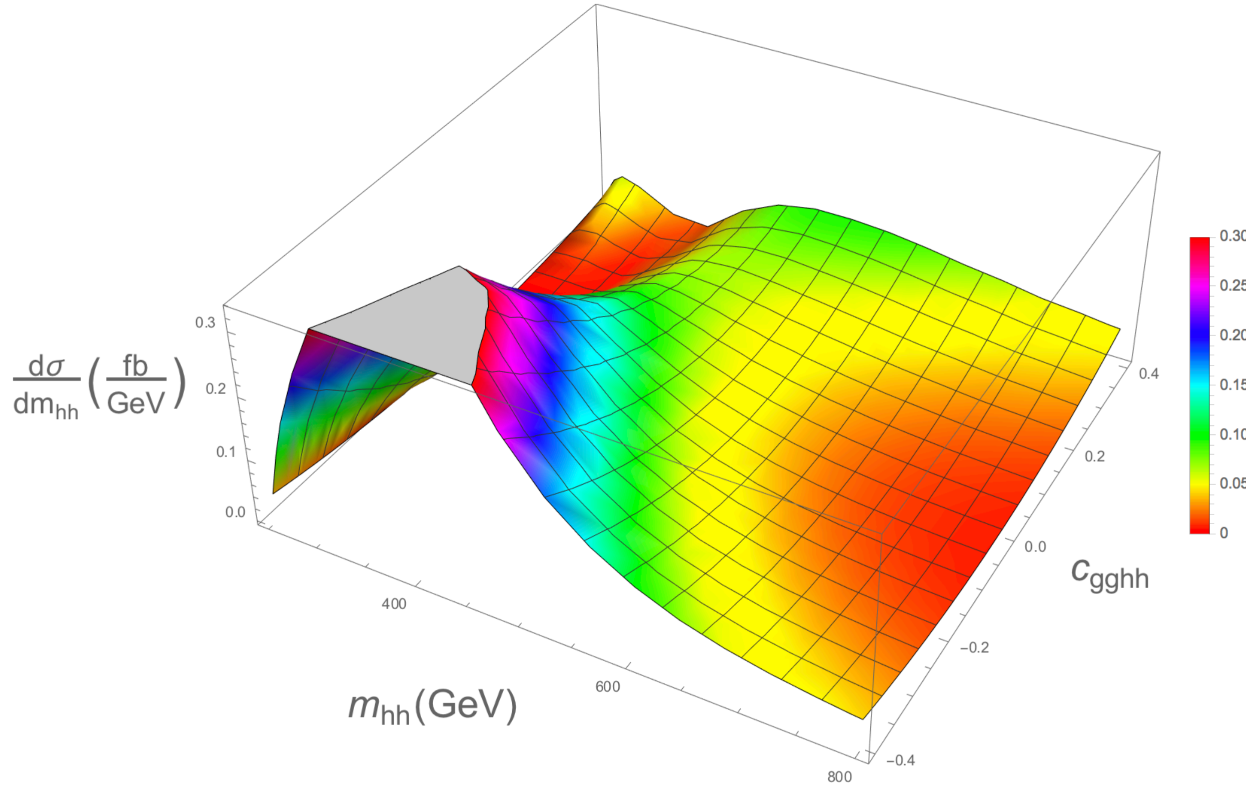
$\frac{d\sigma}{dm_{hh}}\left(\frac{fb}{GeV}\right)$
m_{hh}(GeV)
c_{gghh}

Conclusions

- We computed NLO QCD corrections for Higgs boson pair production in the gluon fusion channel within the EWChL framework, working within a five dimensional parameter space.
- We evaluated the full top mass dependent cross sections and differential m_{hh} and p_T distributions for 12 benchmark points up to NLO QCD.
- The analysis shows that in a BSM framework the differential cross section can deviate substantially from the SM prediction or be almost degenerate; studying the differential cross section allows to break the degeneracy.
- We analyzed the total cross section as a function of the five anomalous couplings.
- We studied the behavior of the total and differential cross section as a function of the 3 parameters which are difficult to constrain from other processes.
- We gave a parameterization of the total and differential m_{hh} cross section (available as ancillary files) in terms of 23 coefficients which can allow experimentalists to make further analysis.


BACKUP SLIDES

Virtual contributions to NLO coefficients

- In order to evaluate the virtual coefficients of the parametrization formula we used a different approach.

- In our setup for the virtual corrections we can isolate the contribution of each diagram to the form factors.

- So we can compute each interference and determine directly all the 23 coefficients.

$A_{16} \propto$

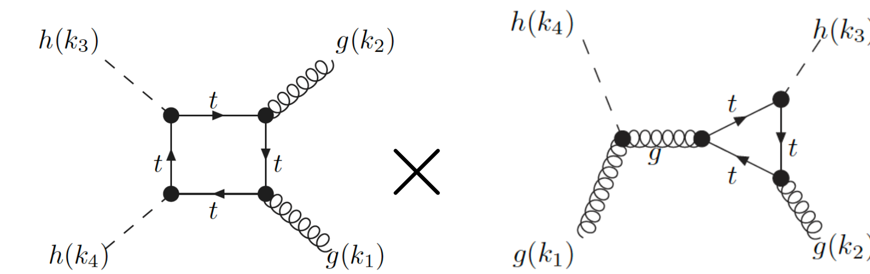

$A_{22} \propto$

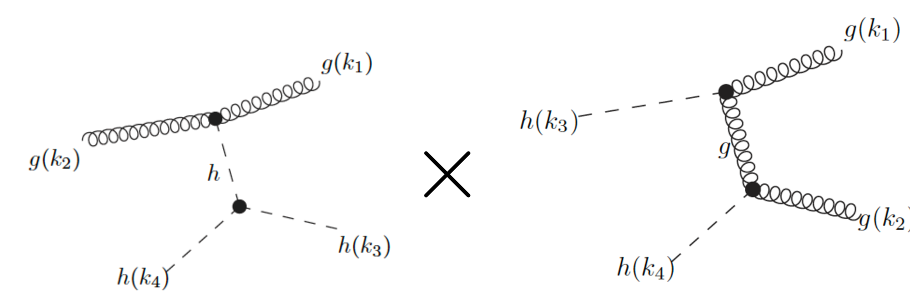

$A_{23} \propto$

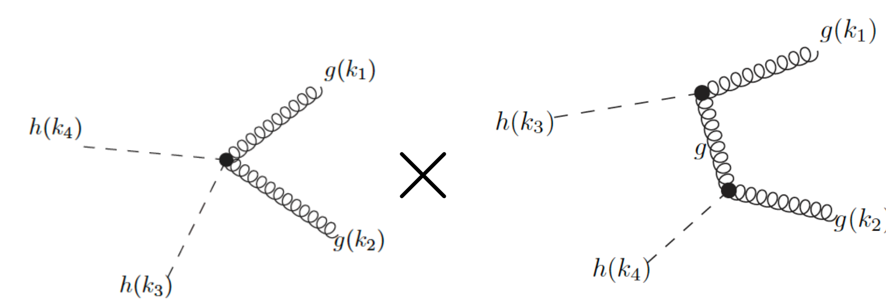

Chromo-magnetic operator

- Operator at least of chiral dimension 4 and loop order 1 and the diagram of loop order 2 but not of order g_s^4.
- Because of the change of chirality and the structure of the lagrangian there is likely one more weak coupling to the new physics sector.
- This would imply loop order 3 and so chiral dimension 6.

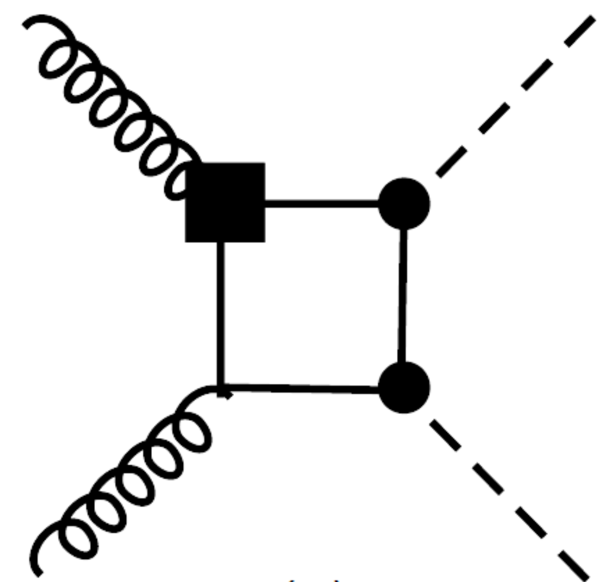

(c)

$$y_t g_s \bar{t}_L \sigma_{\mu\nu} G_{\mu\nu} t_R$$

$$\begin{aligned}\mathcal{L}_2 = & -\frac{1}{2}\langle G_{\mu\nu}G^{\mu\nu}\rangle - \frac{1}{2}\langle W_{\mu\nu}W^{\mu\nu}\rangle - \frac{1}{4}B_{\mu\nu}B^{\mu\nu} + \sum_{\psi=q_L,l_L,u_R,d_R,e_R} \bar{\psi} i \not{D} \psi \\ & + \frac{v^2}{4}\langle D_\mu U^\dagger D^\mu U\rangle \left(1 + F_U(h)\right) + \frac{1}{2}\partial_\mu h \partial^\mu h - V(h) \\ & - v\left[\bar{q}_L \left(Y_u + \sum_{n=1}^{\infty} Y_u^{(n)} \left(\frac{h}{v}\right)^n\right) U P_+ q_R + \bar{q}_L \left(Y_d + \sum_{n=1}^{\infty} Y_d^{(n)} \left(\frac{h}{v}\right)^n\right) U P_- q_R \right. \\ & \left. + \bar{l}_L \left(Y_e + \sum_{n=1}^{\infty} Y_e^{(n)} \left(\frac{h}{v}\right)^n\right) U P_- l_R + \text{h.c.}\right] . \qquad (2.1)\end{aligned}$$